OPEN

Citation: Oncogenesis (2014) **3**, e119; doi:10.1038/oncsis.2014.33

www.nature.com/oncsis

ORIGINAL ARTICLE

Targeting filamin B induces tumor growth and metastasis via enhanced activity of matrix metalloproteinase-9 and secretion of VEGF-A

S Bandaru[1], A-X Zhou[1], P Rouhi[2], Y Zhang[2], MO Bergo[3], Y Cao[2,4] and LM Akyürek[1,5]

Filamins regulate cell locomotion and associate with diverse signaling molecules. We have recently found that targeting filamin A (FLNA) reduces RAS-induced lung adenocarcinomas. In this study, we explored the role of another major filamin isoform, filamin B (FLNB), in tumor development. In contrast to FLNA, we report that targeting FLNB enhances RAS-induced tumor growth and metastasis which is associated with higher matrix metallopeptidase-9 (MMP-9) and extracellular signal-regulated kinase (ERK) activity. *Flnb* deficiency in mouse embryonic fibroblasts results in increased proteolytic activity of MMP-9 and cell invasion mediated by the RAS/ERK pathway. Similarly, silencing *FLNB* in multiple human cancer cells increases the proteolytic activity of MMP-9 and tumor cell invasion. Furthermore, we observed that *Flnb*-deficient RAS-induced tumors display more capillary structures that is correlated with increased vascular endothelial growth factor-A (VEGF-A) secretion. Inhibition of ERK activation blocks phorbol myristate acetate-induced MMP-9 activity and VEGF-A secretion *in vitro*. In addition, silencing *FLNB* in human ovarian cancer cells increases secretion of VEGF-A that induces endothelial cells to form more vascular structures *in vitro*. We conclude that FLNB suppresses tumor growth and metastasis by regulating the activity of MMP-9 and secretion of VEGF-A which is mediated by the RAS/ERK pathway.

Oncogenesis (2014) **3,** e119; doi:10.1038/oncsis.2014.33; published online 22 September 2014

INTRODUCTION

Increased tumor growth and metastasis during tumor progression is highly dependent on oncogenic angiogenesis and degradation of the extracellular matrix. The ectopic expression of metalloproteinases (MMPs) and pro-angiogenic growth factors including vascular endothelial growth factor (VEGF) is a common phenomenon in multiple cancers. Drugs counteracting these processes such as antiangiogenic drugs and MMP inhibitors have been intensively studied as cancer therapeutics.[1,2] However, the clinical usage of these drugs is currently limited by the moderate beneficial effects or high toxicities.[1,2] The identification of novel molecules that regulate tumor angiogenesis and matrix invasion will therefore provide valuable mechanistic insights, thus promoting the design of new anticancer therapies.

Filamins (FLNs) are large actin-binding proteins consisting of three conserved isoforms in mammals: FLNA, FLNB and FLNC. FLNs crosslink cortical cytoplasmic actin filaments into a dynamic three-dimensional structure and anchor the actin network onto the plasma adhesion receptors such as integrins, thus regulating the dynamic changes of the actin cytoskeleton in response to extracellular signals. On the other hand, FLNs also regulate the activity of integrins and their ligand binding. Moreover, FLNs interact with diverse cellular proteins, including transmembrane receptors, ion channels, signaling molecules and transcription factors that may directly or indirectly regulate cellular response and cell motility.[3–5] Recently, the aberrant expression or intracellular localization of FLNA has been clinically associated with the aggression of multiple cancers, including hepatic cholangiocarcinoma,[6] pancreatic cancer,[7] prostate cancer,[8] metastatic breast cancer and high-grade astrocytoma.[9] We and others have found that targeting FLNA reduces RAS-induced lung tumors in mice[10] and *Flna* deficiency causes significant reduction in lung, splenic and systemic metastasis of tumor cells in nude mice.[11] This suggests that FLNA positively regulates tumor progression either through its essential function in cell locomotion or its scaffolding functions in cell signaling. Because of its profound effect on cancers, FLNA seems to be an important disease marker in certain cancers and a potential therapeutic target.[8,9,12,13]

FLNB shares 80% amino acid sequence homology with FLNA and the potential functional compensation between the two isoforms has been under recent debate.[14,15] Despite the high homology between the two isoforms, either *Flna* or *Flnb* deficiency causes severe distinct developmental malformations in genetic mouse models.[16–20] In humans, mutations of either isoform associate with severe genetic diseases, indicating that FLNA and FLNB have equally distinguished biological functions and cannot completely compensate each other during organ development.[5] In contrast to the intensive research efforts on the tumor biology of FLNA, the functions of FLNB in tumor cell signaling and growth are barely explored. Hence, it is becoming urgent to study the role of FLNB in tumor development to get a

[1]Department of Medical Biochemistry and Cell Biology, Institute of Biomedicine, University of Gothenburg, Göteborg, Sweden; [2]Department of Microbiology, Tumor and Cell Biology, Karolinska Institute, Stockholm, Sweden; [3]The Sahlgrenska Cancer Center, University of Gothenburg, Göteborg, Sweden; [4]Department of Medicine and Health Sciences, Linköping University, Linköping, Sweden and [5]Department of Clinical Pathology and Genetics, The Sahlgrenska University Hospital, Göteborg, Sweden. Correspondence: Professor LM Akyürek, Department of Medical Biochemistry and Cell Biology, Institute of Biomedicine, University of Gothenburg, Medicinaregatan 9A, SE-405 30 Göteborg, Sweden.
E-mail: levent.akyurek@gu.se
Received 15 May 2014; revised 29 July 2014; accepted 4 August 2014

comprehensive understanding of FLNs in tumors and provide a potential diagnostic and therapeutic usage of FLNs.

The goal of this study is to investigate the role of FLNB in local growth and metastasis during tumorigenesis. Using inoculation of H-RAS-transformed *Flnb*-deficient mouse embryonic fibroblasts (MEFs), we report that *Flnb*-deficient tumor cells gained enhanced capability to form larger tumors in mice and to disseminate in zebrafish embryo bodies. The *Flnb*-deficient tumors also displayed more angiogenic structures. This suggests that FLNB actually plays a suppressive role in tumor progression.

RESULTS

Flnb deficiency promotes tumor growth and metastasis

Rapid tumor growth and enhanced metastasis are the two major characteristics in tumor progression. To study the role of FLNB in tumor growth, we transformed $Flnb^{+/+}$ and $Flnb^{-/-}$ MEF with H-RAS oncogene. The level of transformed H-RAS was similar between all $Flnb^{+/+}$ and $Flnb^{-/-}$ MEF clones and one representative clone was illustrated (Figures 1a and b). Both H-RAS-transformed (H-RAS$^+$) $Flnb^{+/+}$ and $Flnb^{-/-}$ cells proliferate faster than wild-type controls ($Flnb^{+/+}$H-RAS$^-$), indicating that H-RAS transformation induced cell proliferation (Figure 1c). In addition, the rate of proliferation was faster in $Flnb^{-/-}$ H-RAS$^+$ cells than in $Flnb^{+/+}$*H-RAS*$^+$ cells. We have then inoculated the oncogenic $Flnb^{+/+}$ and $Flnb^{-/-}$ MEF into severe combined immunodeficient (SCID) mice. The tumor volume was periodically measured for up to 13 days. Remarkably, $Flnb^{+/+}$ tumors stopped growing after 7 days of inoculation, whereas $Flnb^{-/-}$ tumors continuously grew over time and were more than two fold larger than $Flnb^{+/+}$ tumors at day 13 (Figure 1d). To assess the effect of FLNB deficiency on tumor metastasis, we adopted a recently developed metastatic model in zebrafish that allows analysis of tumor cell dissemination at the single-cell level.[21] Fluorescently labeled H-RAS-transformed $Flnb^{+/+}$ and $Flnb^{-/-}$ MEF were implanted into the perivitelline cavity of 48 h post fertilized zebrafish embryos. The tumor cells and foci that were disseminated into head/trunk and tail regions of zebrafish embryos were assessed 6 days after implantation (Figures 2a–d). Implantation of $Flnb^{-/-}$ MEF led to a significantly higher number of disseminated cells and foci in zebrafish embryos (Figure 2e), indicating that *Flnb* deficiency leads to increased cell metastasis.

FLNB attenuates phorbol ester-induced MMP-9 expression and activity in fibroblasts

FLNA has been previously reported to suppress the production of either MMP-9 or MMP-2,[22] the essential factors in tumor metastasis. To determine whether the induced metastasis in *Flnb*-deficient tumor cells is related to extracellular matrix degradation, we analyzed the expression and proteolytic activity of MMP-9 and MMP-2 in $Flnb^{+/+}$ and $Flnb^{-/-}$ MEFs. Serum-starved $Flnb^{+/+}$ and $Flnb^{-/-}$ MEFs were treated with or without phorbol myristate acetate (PMA), a tumor promoter that is known to induce MMP expression. The expression of *Mmp9* in both $Flnb^{+/+}$ and $Flnb^{-/-}$ MEFs was significantly induced by PMA. However, the response to PMA induction in the expression of *Mmp9* was higher in $Flnb^{-/-}$ MEF than in $Flnb^{+/+}$ MEFs (Figure 3a). In contrast, the mRNA expression of *Mmp2* was not induced by PMA in either $Flnb^{+/+}$ or $Flnb^{-/-}$ MEFs (Figure 3b), suggesting FLNB differentially regulates expression of *Mmp9* and *Mmp2* at the mRNA level in MEFs.

The proteolytic activity of MMP-9 and MMP-2 was analyzed by gelatin zymography. Consistent with the mRNA expression, the baseline proteolytic activity of MMP-9 and MMP-2 showed similar levels between $Flnb^{+/+}$ and $Flnb^{-/-}$ MEFs. However, *Flnb* deficiency significantly enhanced PMA-induced proteolytic activity of MMP-9 in $Flnb^{-/-}$ cells, but not in $Flnb^{+/+}$ cells (Figure 3c). Similar to the unchanged expression of *Mmp2* mRNA, the proteolytic activity of MMP-2 was not regulated by PMA in either $Flnb^{+/+}$ or $Flnb^{-/-}$ MEFs (Figure 3d).

To assess the functional importance of increased activity of MMP-9, we analyzed the invasion capability of $Flnb^{+/+}$ and $Flnb^{-/-}$ MEFs stimulated with or without PMA in a matrigel invasion assay (Figure 3e). The number of invaded $Flnb^{-/-}$ MEFs was significantly

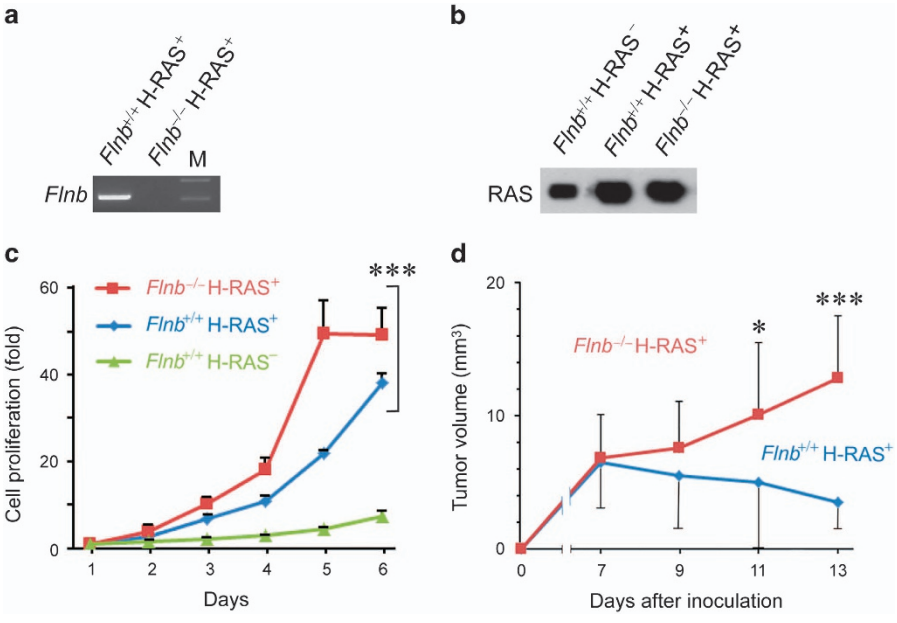

Figure 1. H-RAS-transformed *Flnb*-deficient fibroblasts form larger tumors in SCID mice. (**a**) Genotyping of wild-type ($Flnb^{+/+}$) and *Flnb*-deficient ($Flnb^{-/-}$) MEFs transfected with plasmid encoding H-RAS. (**b**) Immunoblots of total RAS expression in $Flnb^{+/+}$ and $Flnb^{-/-}$ cells transfected with plasmid encoding H-RAS (H-RAS$^+$) and nontransfected cells (H-RAS$^-$). (**c**) Number of $Flnb^{-/-}$H-RAS$^+$, $Flnb^{+/+}$H-RAS$^+$ and $Flnb^{+/+}$ H-RAS$^-$ (wild-type) MEF cells assayed for proliferation. (**d**) Volume of $Flnb^{-/-}$H-RAS$^+$ and $Flnb^{+/+}$H-RAS$^+$ tumors inoculated into SCID mice up to 13 days ($n = 12$ in each group). Data are expressed as mean ± s.d. *$P < 0.05$; ***$P < 0.001$ versus $Flnb^{+/+}$H-RAS$^+$ cells or tumors.

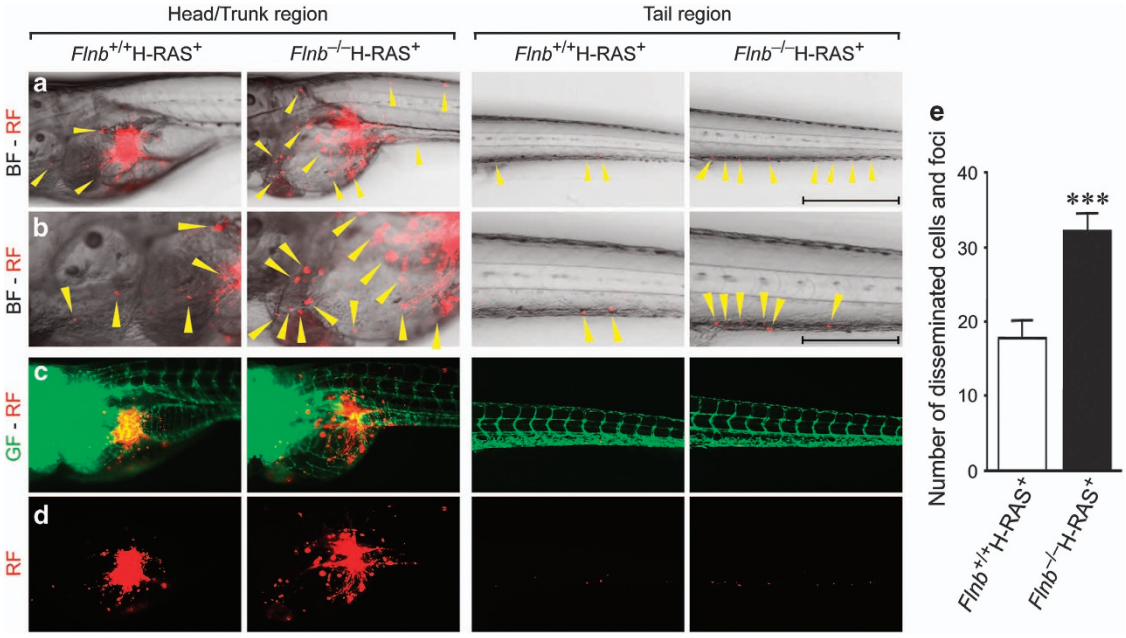

Figure 2. H-RAS-transformed *Flnb*-deficient fibroblasts metastasize more actively in zebrafish. H-RAS-transformed wild-type ($Flnb^{+/+}$H-RAS$^+$) and homozygous filamin B-deficient ($Flnb^{-/-}$H-RAS$^+$) MEFs were labeled with red fluorescent (RF) dye before implantation and were implanted into the perivitelline cavity of 48 h post fertilized zebrafish embryos. Tumor cells and foci were disseminated into head/trunk and tail regions of the zebrafish embryos 6 days post implantation. Yellow arrowheads indicate disseminated cells and foci. (**a**) Bright field (BF) image of the head/trunk and tail of zebrafish embryo merged with RF image of the tumor cells (4×, scale bar, 500 μm). (**b**) Higher magnification of head/trunk and tail regions with metastatic cells pointed by arrowheads (scale bar, 250 μm). (**c**) Vasculature of the transgenic zebrafish embryo strain expressing enhanced green fluorescent (GF) protein under the *fli1* promoter where RF dyed tumor cells and foci are disseminated into proximal and distal parts of the fish body (4×). (**d**) Primary tumor mass and disseminated tumor cells and foci (4×). (**e**) Number of disseminated $Flnb^{+/+}$H-RAS$^+$ and $Flnb^{-/-}$H-RAS$^+$ cells in the entire zebrafish. Data are expressed as mean ± s.d. ***$P < 0.001$.

increased in response to PMA as compared with response of $Flnb^{+/+}$ MEFs to PMA.

Induction of MMP-9 in $Flnb^{-/-}$ MEFs and tumors is mediated by the MAPK cascade

One important pathway that responds to extracellular stimuli and regulates MMP-9 expression is the mitogen-activated protein kinase (MAPK) cascade. Among the subgroups of the MAPK cascade, the extracellular signal-regulated kinase-1/2 (ERK1/2) signaling pathway is preferentially activated in response to growth factors and PMA. To assess whether the MAPK cascade was differentially affected by PMA stimulation between $Flnb^{+/+}$ and $Flnb^{-/-}$ MEFs, the activation of RAS-GRF, various PKC isoforms and ERK1/2 was examined by immunoblotting (Figure 4a). $Flnb^{-/-}$ MEFs displayed increased levels of RAS-GRF, and phosphorylated ERK1/2 in response to PMA stimulation (Figure 4a). Levels of FLNA protein were not different between $Flnb^{+/+}$ and $Flnb^{-/-}$ MEFs with or without PMA stimulation, indicating that FLNA expression was not altered to compensate for the lack of FLNB in our cellular model (Figure 4a).

In the MAPK cascade, MAPK kinase (MEK) directly phosphorylates ERK1/2 and leads to its activation. To determine whether the proteolytic activity of MMP-9 was dependent on ERK1/2 signaling, the proteolytic activity of PMA-stimulated MEFs was measured after pretreatment with PD 098059, a specific MEK inhibitor that preferentially blocks ERK1/2 phosphorylation (Figure 4b). Pretreatment with this inhibitor abolished the PMA-induced MMP-9 activity in $Flnb^{-/-}$ MEFs (Figure 4c), whereas the proteolytic activity of MMP-2 was not affected (data not shown).

In agreement with our *in vitro* study, the remarkably increased tumor growth in $Flnb^{-/-}$ tumors was associated with significantly induced MMP-9 production and ERK activation *in vivo* (Figures 4d and e). These results suggest that the increased invasion capability *in vitro* and the enhanced metastasis *in vivo* of *Flnb*-deficient tumor cells are likely mediated by MAPK/ERK cascade-regulated MMP-9 expression.

FLNB suppresses MMP-9 expression in endothelial and tumor cells

To validate our finding in MEFs that FLNB suppresses MMP-9 expression is ubiquitous, we evaluated MMP-9 expression or proteolytic activity in either primary embryonic endothelial cells (ECs) isolated from $Flnb^{+/+}$ and $Flnb^{-/-}$ mice or human tumor cells with targeted FLNB silencing by FLNB small hairpin RNA (shRNA). *Mmp9* mRNA levels were significantly increased in $Flnb^{-/-}$ ECs in normal culture condition with serum, indicating that FLNB constitutively suppresses *Mmp9* expression (Figure 5a). Moreover, transient FLNB silencing in M2 human melanoma cells (Figure 5b) resulted in a significant increase in *MMP9* mRNA expression (Figure 5c), further excluding the possibility that increased MMP9 expression is because of a developmental compensation for FLNB deficiency. FLNA has been previously reported to decrease MMP-9 expression in human melanoma cells.[22] Thus, our finding in *FLNA*-deficient M2 cells suggested that the suppressive effect of FLNA and FLNB on MMP-9 expression is synergetic, although in some cases the two FLN isoforms can compensate for each other functionally.[5] Furthermore, the proteolytic activity of MMP-9 was significantly increased when FLNB was silenced in human ovarian cancer cells (Figures 5d and e) that is associated with enhanced cancer cell invasion (Figure 5f).

Flnb deficiency enhances tumor angiogenesis and induces VEGF-A secretion that is likely mediated by the MAPK cascade

Tumors induce angiogenesis by secreting growth factors including VEGF-A that is a fundamental step in the malignant transformation of tumors. We assessed capillary structures in tumors formed from H-RAS-transformed $Flnb^{+/+}$ and $Flnb^{-/-}$ MEFs in SCID mice. The

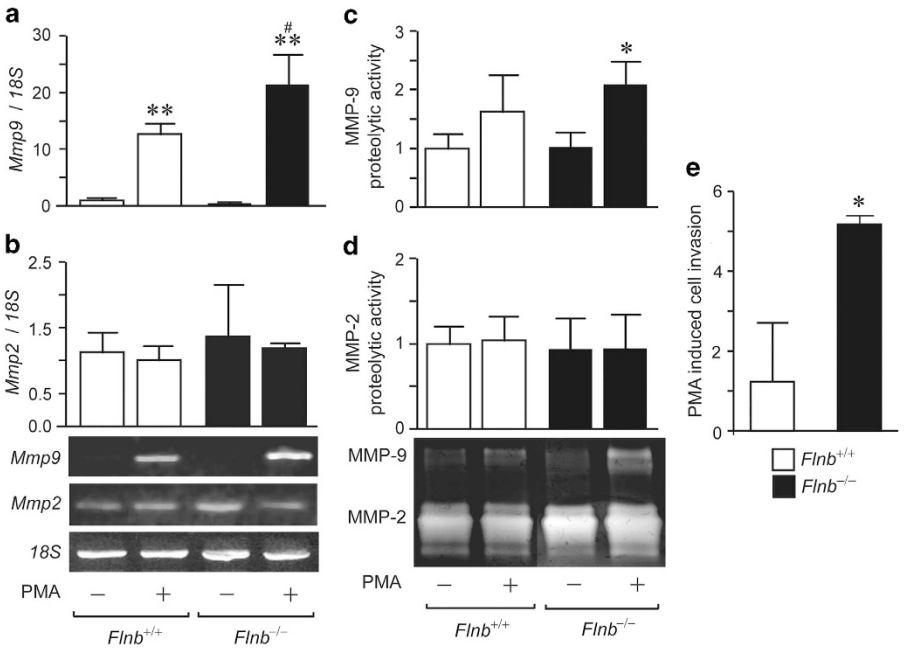

Figure 3. Increased expression of *Mmp9* mRNA and MMP-9 proteolytic activity in MEFs deficient for FLNB. Semiquantitative analysis of *Mmp9* (**a**) and *Mmp2* (**b**) mRNA in wild-type ($Flnb^{+/+}$) and *Flnb*-deficient ($Flnb^{-/-}$) MEFs as detected by reverse transcriptase–PCR (RT–PCR) and normalized to *18S* mRNA. Cells were serum starved and treated with or without PMA. Representative images of gel electrophoresis are shown. Quantification of the proteolytic activity of MMP-9 (**c**) and MMP-2 (**d**) in cell culture medium by gelatin zymography. Representative images of zymography. (**e**) Invasion of $Flnb^{+/+}$ and $Flnb^{-/-}$ MEFs in response to PMA stimulation. $Flnb^{+/+}$ and $Flnb^{-/-}$ MEFs were cultured with PMA in serum-starved conditions and assayed for cell invasion through a Matrigel-coated Boyden chamber. Fold changes in the number of cells invaded through the Matrigel-coated membrane. Data of triplicated experiments are expressed as mean ± s.d. $^{*}P < 0.05$; $^{**}P < 0.01$ versus non-PMA-treated respective MEFs; $^{\#}P < 0.05$ *versus* PMA-treated $Flnb^{+/+}$ MEFs.

$Flnb^{-/-}$ tumors displayed an obviously different morphology compared with $Flnb^{+/+}$ tumors. The number of vasculatures was increased whereas the vasculature network was more disorganized in $Flnb^{-/-}$ tumors (Figure 6a). Correspondingly, the $Flnb^{-/-}$ tumors secreted significantly higher levels of VEGF-A than $Flnb^{+/+}$ tumors (Figure 6b). To assess whether this induced VEGF-A secretion is mediated by the MAPK cascade, we measured secreted VEGF-A in cultured medium of H-RAS-transformed $Flnb^{+/+}$ and $Flnb^{-/-}$ MEFs. $Flnb^{-/-}$ MEFs secreted more VEGF-A and their secretion of VEGF-A was more remarkably enhanced upon PMA treatment compared with $Flnb^{+/+}$ MEFs. However, the addition of MAPK inhibitor significantly decreased the secretion of VEGF-A in these cells, indicating that the majority of induced VEGF-A was mediated by the MAPK pathway (Figure 6c).

Flnb silencing in tumor cells induces VEGF-A secretion and *in vitro* angiogenesis

In agreement to our finding in H-RAS-transformed MEFs, silencing of FLNB in human ovarian cancer cells also significantly induced the secretion of VEGF-A (Figure 6d). Importantly, the conditioned medium collected from FLNB-silenced ovarian cancer cell cultures significantly promoted the formation of vasculature-like circular structures of porcine aortic endothelial cells in a matrigel angiogenesis assay compared with normal ovarian cancer cell culture medium (Figure 6e). These results provide further evidence that FLNB suppresses VEGF-A secretion in tumors that could regulate the angiogenic process.

DISCUSSION

In contrast to the stimulatory role of FLNA in tumor progression, we surprisingly found that the absence of FLNB actually promotes tumor growth. Our study revealed that the induced progression of *Flnb*-deficient tumors is likely mediated by increased metastasis and angiogenesis. We further explored the molecular mechanism that the enhanced tumor metastasis and angiogenesis may be mediated by an MAPK/ERK pathway-dependent increase in MMP-9 expression and VEGF-A secretion in *Flnb*-deficient tumor cells. This unanticipated finding suggests a differential role of FLNA and FLNB in tumor development.

FLNs are widely considered to be crucial for cell motility by either directly modulating the actin cytoskeleton or scaffolding for other signaling molecules. *FLNA*-deficient human melanoma cells and $Flnb^{-/-}$ MEFs exhibit remarkably reduced cell migration.[18] In contrast to our current understanding of the role of FLNs in cell migration, $Flnb^{-/-}$ tumor cells displayed enhanced metastasis in our zebrafish model. $Flnb^{-/-}$ tumor cells also displayed enhanced invasive capability *in vitro*. Cell metastasis and invasion is a complex process that involves both cell migration and degradation of the extracellular matrix. Interestingly, *FLNA*-deficient melanoma cells and megakaryocytes displayed an increased expression and activity of MMP-9.[22,23] Contradictory to these studies, a recent report showed that both *FLNA* and *FLNB* knockdown activated MMP-2 but not MMP-9 in human fibrosarcoma cells, leading to enhanced extracellular matrix degradation.[24] We found that expression of MMP-9 was induced in $Flnb^{-/-}$ mouse fibroblasts and ECs, and in *FLNB*-knockdown human melanoma and ovarian cancer cells. The discrepancy between the different effects on MMPs by FLNs might be cell-type specific. For example, in contrast to human melanoma cells where the proteolytic activity of MMP-2 is very low,[22] the proteolytic activity of MMP-2 was markedly higher than MMP-9 in both $Flnb^{+/+}$ and $Flnb^{-/-}$ MEFs in our study. This indicates that the expression of MMP-2 and -9 have differential regulation in a cell type-specific manner. The differences can be linked to the promoter elements of *MMP2* and *MMP9*. The promoter of *MMP9* is similar to most other MMPs, whereas the MMP-2 promoter lacks many of the

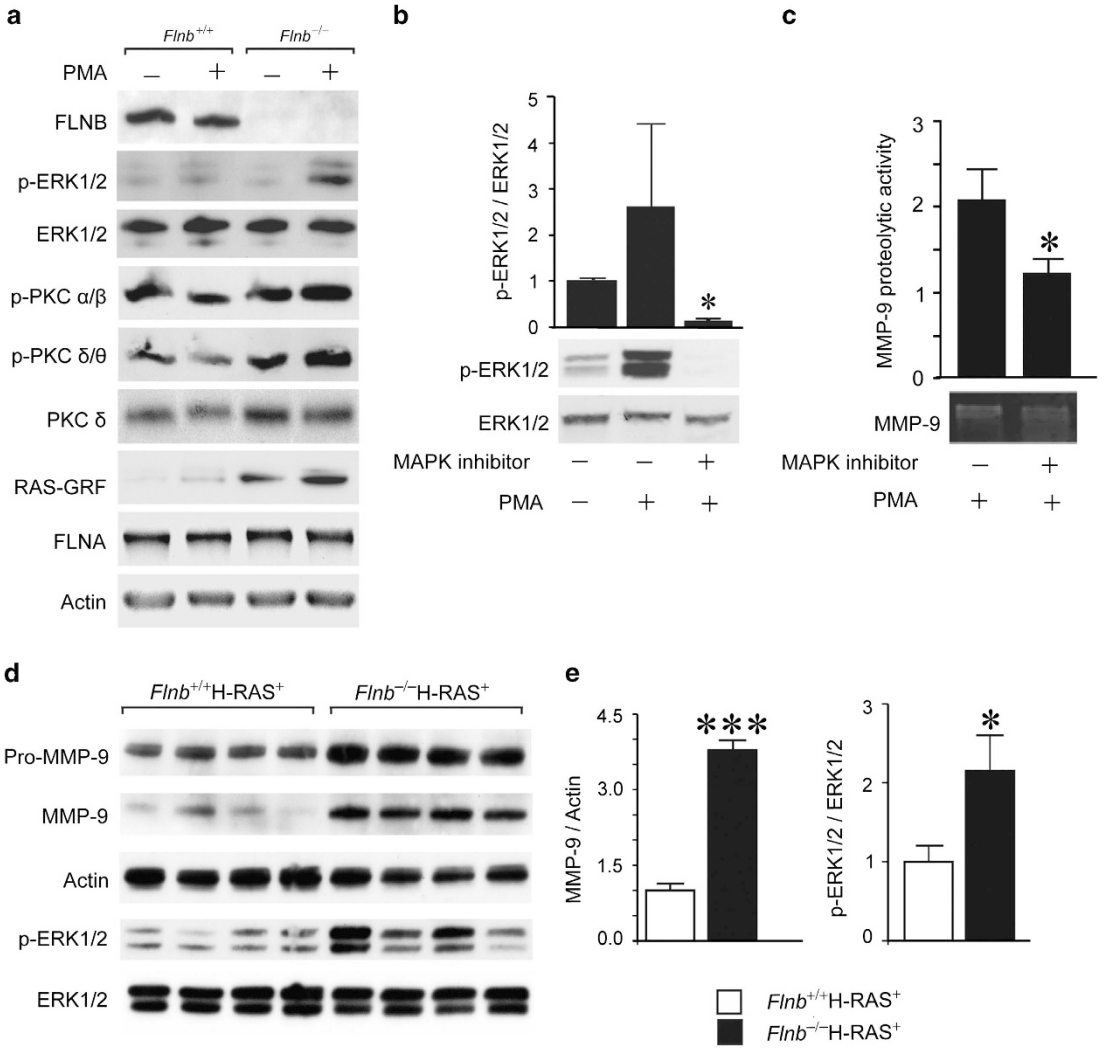

Figure 4. The MAPK cascade mediates PMA-induced MMP-9 proteolytic activity in cells deficient for FLNB. (**a**) Representative immunoblots detecting protein levels of FLNB, RAS-GRF, phosphorylated PKC-α/β, phosphorylated PKC-δ/θ, total PKC-δ, phosphorylated ERK1/2, total ERK1/2 and FLNA in serum-starved $Flnb^{+/+}$ and $Flnb^{-/-}$ MEFs after induction with or without PMA for 15 min. Actin served as an internal loading control. (**b**) Representative immunoblot demonstrating the inhibition of p-ERK1/2 expression in $Flnb^{-/-}$ cells induced with PMA and pretreated with PD 098059, a MAPK inhibitor. $^{*}P < 0.05$ *versus* non-pretreated MEF with PD 098059. (**c**) Gelatin zymography detecting proteolytic activity of MMP-9 in cell culture medium of $Flnb^{-/-}$ MEFs pretreated with PD 098059, and then cultured in serum-starved conditions with PMA. (**d**) Immunoblots for pro-MMP-9, MMP-9, p-ERK1/2 and total ERK1/2 proteins extracted from $Flnb^{-/-}$H-RAS^{+} and $Flnb^{+/+}$H-RAS^{+} tumors. Actin served as an internal loading control. (**e**) Densitometric reading of MMP-9 and p-ERK1/2 proteins are given as fold differences. Data of triplicate or quadruplicate experiments are expressed as mean ± s.d. $^{*}P < 0.05$; $^{***}P < 0.001$ versus non-PD 098059-treated MEFs or $Flnb^{+/+}$H-RAS^{+} tumors.

inducible promoter elements such as binding sites for the AP-1 and ETS transcription factors.[25] Nevertheless, these findings raise an important issue that cell metastasis may be dependent on the balance between cell motility and MMP expression and activity that are regulated by FLNs. Although most of the studies point to a positive correlation between expression of FLNA and metastasis in cancers, two recent studies showed that FLNA expression is negatively correlated with the malignancy of breast cancer lines.[26,27] This is probably because of the suppression of FLNA on breast cancer cell migration and invasion. It is interesting that *FLNA*-deficient cells show reduced migration, but induced expression of MMPs. This also makes it complicated to predict the final effect on tumor metastasis. We and others have found that *in vivo Flna* deficiency caused tumor growth in lung cancer and other cancers. This indicates that reduced cell migration may overcome the overexpression of MMPs in certain *Flna*-deficient tumor cells. However, in a metastasis assay, *Flnb*-deficient tumor cells displayed enhanced spreading of tumor cells. It still requires further investigation regarding how the similar phenotypes of *FLNA*- and *FLNB*-deficient cells display opposite outcomes *in vivo*. Nevertheless, our findings may reflect a dual role of FLNs in tumor invasion: in one aspect, FLNs are critical for cell migration and deficiency of FLNs may impair tumor invasion; in another aspect, FLNs inhibit MMP activity that may suppress tumor invasion. The dual role of FLNs in tumor invasion may depend on the stages of tumor progression or work coordinately in regulating tumor metastasis.

Tumor growth is highly dependent on angiogenesis for sufficient blood flow supply. In the absence of angiogenesis, tumor implants do not grow beyond 2 to 3 mm^3 and enter into a dormant state.[28] We found that *Flnb*-deficient tumors secrete more VEGF-A and display enhanced angiogenesis that likely accounts for the continuous growth of *Flnb*-deficient tumors compared with the *Flnb*-expressing tumors. Oncogenic

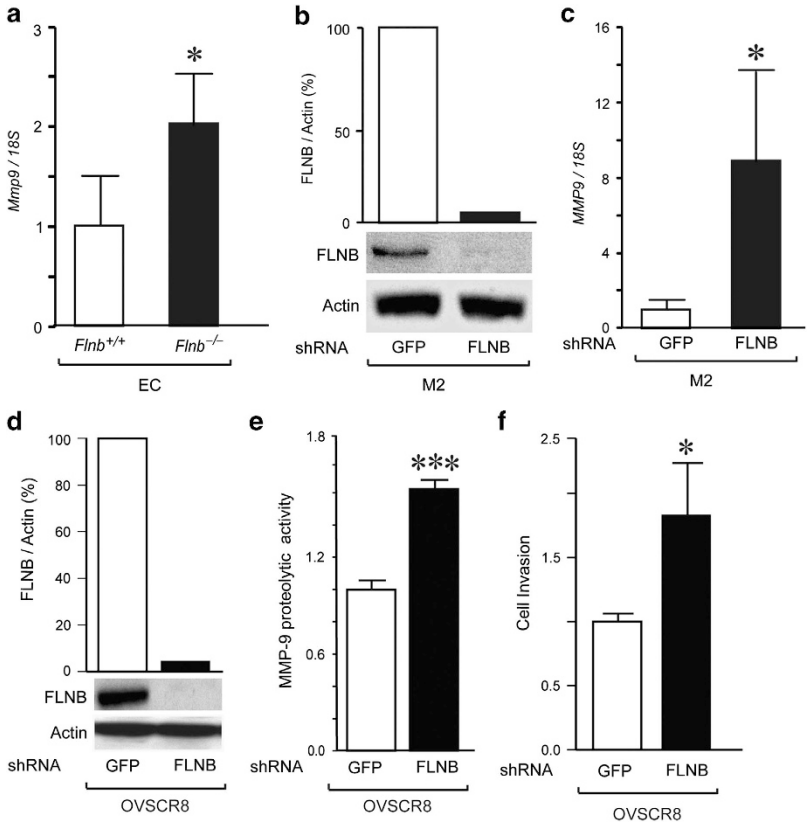

Figure 5. Increased *MMP9* mRNA expression in vascular endothelial and tumor cells in the absence of FLNB. (**a**) *Mmp9* mRNA expression in mouse embryonic filamin B-deficient ($Flnb^{-/-}$) ECs as compared with wild-type ($Flnb^{+/+}$) ECs as detected by reverse transcriptase–PCR (RT–PCR). (**b**) FLNB protein expression in human melanoma M2 cells as detected by immunoblots after transfection with vector expressing FLNB shRNA. Immunoblot with Actin served as loading controls. Transfection with GFP shRNA was included as a negative control. (**c**) Increased mRNA expression of *MMP9* in *FLNB*-silenced M2 cells. (**d**) FLNB protein expression in OVSCR8 cells transfected with FLNB shRNA, whereas same cells transfected with GFP shRNA served as negative controls. (**e**) Proteolytic activity of MMP-9 in human ovarian cancer OVSCR8 cells following transfection with FLNB or GFP shRNA. (**f**) Invasion of OVSCR8 cells after transfection with FLNB or GFP shRNA. Data of triplicated experiments are expressed as mean ± s.d. $^{*}P < 0.05$; $^{***}P < 0.001$ versus respective controls.

angiogenesis is a highly integrated system involving the secretion of angiogenic factors by malignant tumor cells, causing ECs to proliferate, migrate and sprout in response.[1] The impact of FLNs on angiogenesis has been recently revealed by findings that ECs display reduced migratory and angiogenic activity after *FLNA* or *FLNB* silencing.[29,30] This supports our previous finding that EC-specific deficiency of FLNA reduces subcutaneous fibrosarcoma growth and vascularity within tumors.[10] However, in the mouse model using tumor inoculation that we used in this study, the ECs are derived from the wild-type host mice. Thus, the increased angiogenesis in *Flnb*-deficient fibrosarcomas is likely because of the altered production of angiogenic factors from *Flnb*-deficient tumor cells. In our study, we found that *Flnb*-deficient mouse fibrosarcoma cells and *FLNB*-knockdown human ovarian cancer cells secrete more VEGF-A. This provides a potential mechanistic explanation for enhanced angiogenesis in *Flnb*-deficient tumors. In contrast to FLNB in this study, we recently identified hypoxia-inducible factor-1α as an interacting partner of FLNA, and absence of FLNA in melanoma cells leads to significantly reduced VEGF-A secretion.[31] In contrast to FLNB in this study, *FLNA*-deficient tumor cells secrete significantly less level of VEGF-A. A brief clinical report identified that the expression of FLNA positively correlates with the VEGF-A level in human lung tumors.[32] This implies that FLNA may positively regulate VEGF-A production. Further investigation is required to clarify whether FLNA and FLNB regulate VEGF-A production through different pathways or deficiency of FLNB may actually release FLNA from their heterodimer structure, thus enhancing the activity of FLNA in this particular scenario.

Cytokines and growth factors that activate MMP-9 expression typically act via the MAPK cascade including the ERK1/2 signaling pathway.[25] Our study showed that PMA-induced activation of ERK1/2 was lower in $Flnb^{+/+}$ MEFs, suggesting that FLNB suppresses the ERK1/2 signaling pathway and thus leads to less expression of MMP-9. PMA is a direct activator of PKC proteins that are upstream in the MAPK cascade. PMA-stimulated expression of MMP-9 was abolished in $Flnb^{+/+}$ MEFs, indicating that FLNB may interfere with protein kinase C (PKC) activity. PKC is a family of protein kinases consisting of conventional (PKC-α, -β_I, -β_{II} and -γ), novel (PKC-δ, -ε, -η and -θ) and atypical (PKC-ι, -ζ, -N1 and -N2) PKC proteins. Thus, to understand how FLNB attenuates the MAPK cascade through PKCs requires the identification of specific PKC isoforms regulated by FLNB. The phosphorylation of both PKC-α/β and PKC-δ/θ was induced by PMA in $Flnb^{-/-}$ MEFs, but not in $Flnb^{+/+}$ MEFs. This implicates a broad function of FLNB in regulating the activity of both conventional and novel PKCs. In spite of FLNB, FLNA can physically associate with PKC-θ and is required for translocation of PKC-θ from the cytosol to the cell membrane.[33] It has also been found that FLNA, but not FLNB, is a ligand and *in vivo* substrate for PKC-α.[34] This indicates that the intimate interaction between FLNs and PKC is both FLN and PKC isoform dependent. The association of FLNB and PKCs may sequester the activation of PKC and thus suppress PMA-induced MAPK cascade activation.

The proteolytic activity of MMP-9 is not only regulated at the gene expression level. The secretion, pro-enzyme activation and presence of specific inhibitors can all regulate its proteolytic

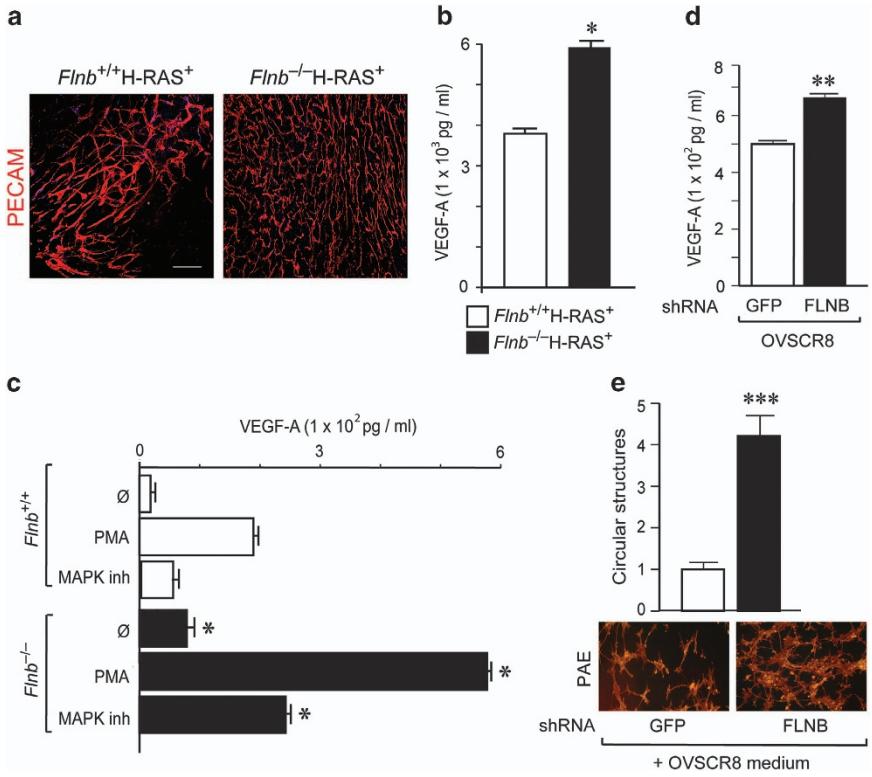

Figure 6. Increased intratumor vascularity because of increased VEGF-A secretion in *Flnb*-deficient tumors *in vivo*. (**a**) Micrographs of vascular networks within mouse tumors formed by H-RAS-transformed MEFs. Red color represents PECAM-positive endothelial cells (scale bar, 100 μm). (**b**) Secreted levels of VEGF-A in mouse H-RAS-transformed wild-type ($Flnb^{+/+}$H-RAS$^+$) or homozygous *Flnb*-deficient ($Flnb^{-/-}$H-RAS$^+$) tumors. (**c**) Secreted levels of VEGF-A in wild-type ($Flnb^{+/+}$) and homozygous *Flnb*-deficient ($Flnb^{-/-}$) MEFs treated without reagent (Ø), PMA or MAPK inhibitor. (**d**) Secreted levels of VEGF in OVSCR8 cells following transfection with FLNB or GFP shRNA. (**e**) Representative image and quantification of circular vascular structures of porcine aortic endothelial (PAE) cells after conditioning with conditioned medium from FLNB or GFP shRNA-transfected OVSCR8 cells. Data of triplicate or quadruplicate experiments are expressed as mean ± s.d. $^*P < 0.05$, $^{**}P < 0.01$ and $^{***}P < 0.001$ versus respective controls.

activity.[35] *Mmp9* mRNA levels in $Flnb^{+/+}$ and $Flnb^{-/-}$ MEFs were both significantly induced upon PMA stimulation, despite $Flnb^{-/-}$ MEFs showing a much higher induction than $Flnb^{+/+}$ MEFs. However, the proteolytic activity of MMP-9 in $Flnb^{+/+}$ MEFs was not regulated by PMA whatsoever. This indicates that other processes in MMP-9 activation are also involved. FLNB may affect the secretion of MMP-9 by regulating transportation vesicles. Another key step in regulating MMP activity is the conversion of the zymogen into an active proteolytic enzyme that is mediated by other activated MMPs or serine proteinases including plasminogen activators. This may represent another potential regulatory level of MMP-9 activity by FLNB. Furthermore, the function of MMPs *in vivo* also depends on the local balance between them and their physiological inhibitors, such as the tissue inhibitors of MMPs.

Analysis of FLNB expression in cancer cohorts shows that FLNB mRNA is downregulated in human colorectal and ovarian cancer, melanomas and gastrointestinal sarcomas (www.oncomine.org, Supplementary Table S1). Protein expression levels and the affected tumor cell signaling remain to be investigated to assess the role of FLNB in these types of cancer. Other roles of FLNB could explain why FLNB is upregulated in some types of cancer (Supplementary Table S2). In summary, our unanticipated findings suggest a differential role of FLNB in tumor development. In contrast to its homolog protein FLNA, FLNB negatively regulates tumor progression by suppressing local growth, angiogenesis and metastasis. Our findings point to the need for delicately designed approaches to target FLNs in tumor diagnosis, progression and treatment.

MATERIALS AND METHODS

Cell cultures

Three different clones of wild-type ($Flnb^{+/+}$) or homozygous *Flnb*-deficient ($Flnb^{-/-}$) MEFs were extracted and cultured as described earlier.[18] VEGFR2-expressing porcine aortic endothelial cells and OVSCR8 cells were cultured in Ham F12 medium and Dulbecco's modified Eagle's medium, respectively, and were supplemented with 10% of fetal bovine serum, 1 × penicillin/streptomycin, 1 × nonessential amino acids and 1 × glutamine at 37 °C in 5% CO_2 cell culture incubators. M2, a human melanoma cell line lacking both *FLNA* mRNA and protein, were cultured as described earlier.[36]

Chemicals

PMA (Sigma-Aldrich, St Louis, MO, USA) and PD 098059 (Sigma Aldrich), a specific inhibitor of MAPK, were used in cell culture studies.

Reverse transcriptase–PCR

Overnight serum-starved MEFs were treated with or without PMA for 6 h. Total RNA from embryonic endothelial cells was isolated at E10.5 as described earlier.[18] The total RNA was isolated by RNeasy mini kit following the manufacturer's instructions (Qiagen Inc., Valencia, CA, USA). The RNA concentration was measured by an Epoch spectrophotometer (Bio-Tek Instruments, Winooski, VT, USA). Complementary DNA was synthesized from 1 μg RNA by the qScript cDNA synthesis kit (Quanta BioSciences, Inc., Gaithersburg, MD, USA). The gene sequences were obtained from National Center for Biotechnology Information (NCBI) and primers were designed by using the primer design tool provided by NCBI (Primer-Blast, Bethesda, MD, USA). The forward primer 5′-GCCTCAAAGAGCTACTGTCCACGAC and reverse primer 5′-GGGTCAGAATCACGCAGGTTACTTT for *Flnb*, 5′-TGGCAGC CCATGAGTTCGGC-3′ and reverse primer 5′-GTGGCCACCAGCAAGGGACC-3′ for *Mmp2* and forward primer 5′-AGCACGGCAACGGAGAAGGC-3′ and

reverse primer 5′-AGCCCAGTGCATGGCCGAAC-3′ for *Mmp9* were purchased from Sigma Aldrich. The PCR conditions were as per instructor manuals (Qiagen Inc.). The corresponding PCR product sizes are *Flnb* (250 kb), *Mmp2* (339 kb), *Mmp9* (389 kb) and *18S* RNA (530 kb). The PCR products were analyzed by 2% agarose gel electrophoresis and quantified by densitometry reading. *18S* RNA was used as an internal loading control for quantification.

Transformations

Three different clones of wild-type ($Flnb^{+/+}$) or homozygous *Flnb*-deficient ($Flnb^{-/-}$) MEFs were transformed with pLXSP3+Human H-RAS (Val12) plasmid expressing H-RAS.[37] All these clones were tested for mRNA expression of *Mmp9* and levels of active RAS. The transformed cells were selected by growing them in antibiotic medium for 2–3 weeks. RAS activity was determined by active RAS pull-down assay (Thermo Fisher Scientific, Waltham, MA, USA).

Tumor cell inoculations

CB17/Icr-Prkdcscid/IcrCrl SCID male mice (Charles River Laboratories International, Inc., Wilmington, MA, USA), 5 to 6 weeks old, were injected subcutaneously with 3×10^6 H-RAS-transformed $Flnb^{+/+}$ MEFs as control group ($n=12$) and $Flnb^{-/-}$ MEFs as test group on the dorsal back region as described earlier.[10] Tumors were carefully harvested, weighed, frozen in liquid nitrogen and stored in −80 °C. All the mouse experiments were approved by the local animal ethical committee.

Zebrafish model of tumor inoculation

A transgenic zebrafish strain expressing enhanced green fluorescent protein (EGFP) under the *fli1* promoter (fli1:EGFP) was used as described earlier.[21] Invasion and dissemination of the tumor cells were investigated 6 days post implantation with a fluorescent microscope (Nikon Instruments Inc., Melville, NY, USA).

Gelatin zymography

$Flnb^{+/+}$ and $Flnb^{-/-}$ MEFs were growth arrested by being cultured in serum-free media overnight at 37 °C. Conditioned media were collected and concentrated with Amicon Ultra-4 centrifugal filter devices (EMD Millipore, Billerica, MA, USA). The enzymatic activity of MMP-9 and MMP-2 was measured by gelatin zymography (Life Technologies, Carlsbad, CA, USA) following instructions provided by the manufacturer. Briefly, after electrophoresis, gels were incubated with 1× renaturation buffer for 30 min followed by overnight incubation in developing buffer at 37 °C. The bands were visualized by simple blue stain for 1 h and destained with distilled water for 1–3 h. The presence of enzyme activity was confirmed by the appearance of white bands on blue background.

Invasion assay

The assay was performed with a Biocoat Matrigel Invasion Chamber (BD Biosciences, San Jose, CA, USA). The experimental procedures were described earlier.[36] The invaded cells were visualized and photographed with a fluorescence microscope (Leica Microsystems, Wetzlar, Germany) and cell number was counted.

Immunoblotting

MEFs were cultured with or without PMA in serum-starved condition overnight. $Flnb^{+/+}$ and $Flnb^{-/-}$ tumor tissues were homogenized and immunoblotted as described earlier,[10] followed by incubation with primary antibody against FLNB (Chemicon International, Inc., Temecula, CA, USA), FLNA (EMD Millipore), Actin (Sigma Aldrich), phosphorylated ERK1/2, total ERK1/2, phosphorylated-PKC-α/β and phosphorylated-PKC-δ/θ (Cell Signaling Technologies, Danvers, MA, USA) and MMP-9 (Nordic BioSite, Taby, Sweden). Membranes were then incubated with an appropriate anti-mouse or anti-rabbit IgG-horseradish peroxide conjugated secondary antibody (Amersham Biosciences, Amersham, UK) and the proteins were visualized by using enhanced chemiluminescence (Amersham Biosciences). The densities of bands were quantified by ImageQuant software (Bio-Rad, Hercules, CA, USA). Actin was used as an internal loading control.

Transfections

M2, A7 and OVSCR-8 cells were transfected with either shRNA GFP or FLNB constructs (SA Biosciences, Frederick, MD, USA) using Fugene HD transfection reagent according to the manufacturer's protocol (Promega, Madison, WI, USA). Transfection efficiency was analyzed by using FLNB immunoblotting (Chemicon International, Inc.).

Fluorescence-activated cell sorting

The shRNA-transfected cells were harvested after 72 h, diluted with 0.5% fetal bovine serum in phosphate-buffered saline and analyzed with fluorescence-activated cell sorting (BD Biosciences). GFP-negative cells were discharged after sorting, and the sorted GFP-positive cells were cultured overnight and were used for experiments the next day.

Enzyme-linked immunosorbent assay

Conditioned medium was collected from cell cultures of wild-type ($Flnb^{+/+}$) or homozygous *Flnb*-deficient ($Flnb^{-/-}$) MEFs, H-RAS-transformed $Flnb^{+/+}$, $Flnb^{-/-}$ MEFs and human ovarian cancer cells (OVSCR-8) assayed for VEGF-A protein according to the manufacturer's protocol (R&D Biosystems, Inc., Minneapolis, MN, USA). VEGF-A levels were measured by an Epoch spectrophotometer (Bio-Tek Instruments).

Matrigel assay

Porcine aortic endothelial cells expressing VEGFR2 were cultured in precoated 24-well plates with Matrigel (BD Biosciences). The cells were cultured until reaching ~50–60% confluency and then conditioned with a mixed medium containing 80% of 2% fetal bovine serum Ham f12 and 20% OVSCR8 cell-conditioned medium. The cells were incubated at 37 °C with 5% CO_2 for 24 h and were fixed with 4% paraformaldehyde for 30 min at room temperature and permeabilized with phosphate-buffered saline with Tween (PBST) 0.01 Triton X-100 for 30 min. Cells were stained with phalloidin (Life Technologies) for 1 h at room temperature followed with 3 washing steps for 10 min. Circular formed structures were photographed (Nikon Instruments Inc.) and counted at five optical fields (10×) for each well.

Statistics

All the values are mean ± s.d. and the difference between the groups was evaluated with a two-tailed Student's *t*-test and considered significant if the *P*-value was <0.05.

CONFLICT OF INTEREST

The authors declare no conflict of interest.

ACKNOWLEDGEMENTS

This work was supported by The Swedish Society of Medicine, The Magnus Bergvall's Foundation, Jubileumfonden, The Sahlgrenska University Hospital, The Royal Society of Arts and Sciences in Göteborg, The Assar Gabrielsson's Foundation, The Swedish Heart and Lung Foundation, The Swedish Research Council and The Swedish Cancer Foundation.

REFERENCES

1 Cao Y, Arbiser J, D'Amato RJ, D'Amore PA, Ingber DE, Kerbel R *et al.* Forty-year journey of angiogenesis translational research. *Science Transl Med* 2011; **3**: 114rv113.
2 Bauvois B. New facets of matrix metalloproteinases MMP-2 and MMP-9 as cell surface transducers: outside-in signaling and relationship to tumor progression. *Biochim Bioph Acta* 2012; **1825**: 29–36.
3 Stossel TP, Condeelis J, Cooley L, Hartwig JH, Noegel A, Schleicher M *et al.* Filamins as integrators of cell mechanics and signalling. *Nat Rev Mol Cell Biol* 2001; **2**: 138–145.
4 Zhou X, Boren J, Akyürek LM. Filamins in cardiovascular development. *Trends Cardiovasc Med* 2007; **17**: 222–229.
5 Zhou AX, Hartwig JH, Akyürek LM. Filamins in cell signaling, transcription and organ development. *Trends Cell Biol* 2010; **20**: 113–123.
6 Guedj N, Zhan Q, Perigny M, Rautou PE, Degos F, Belghiti J *et al.* Comparative protein expression profiles of hilar and peripheral hepatic cholangiocarcinomas. *J Hepatol* 2009; **51**: 93–101.

7 Li C, Yu S, Nakamura F, Yin S, Xu J, Petrolla AA *et al.* Binding of pro-prion to filamin A disrupts cytoskeleton and correlates with poor prognosis in pancreatic cancer. *J Clin Invest* 2009; **119**: 2725–2736.
8 Bedolla RG, Wang Y, Asuncion A, Chamie K, Siddiqui S, Mudryj MM *et al.* Nuclear versus cytoplasmic localization of filamin A in prostate cancer: immunohistochemical correlation with metastases. *Clin Cancer Res* 2009; **15**: 788–796.
9 Alper O, Stetler-Stevenson WG, Harris LN, Leitner WW, Özdemirli M, Hartmann D *et al.* Novel anti-filamin-A antibody detects a secreted variant of filamin-A in plasma from patients with breast carcinoma and high-grade astrocytoma. *Cancer Sci* 2009; **100**: 1748–1756.
10 Nallapalli RK, Ibrahim MX, Zhou AX, Bandaru S, Sunkara SN, Redfors B *et al.* Targeting filamin A reduces K-RAS-induced lung adenocarcinomas and endothelial response to tumor growth in mice. *Mol Cancer* 2012; **11**: 50.
11 Jiang X, Yue J, Lu H, Campbell N, Yang Q, Lan S *et al.* Inhibition of filamin-A reduces cancer metastatic potential. *Int J Biol Sci* 2013; **9**: 67–77.
12 Ai J, Huang H, Lv X, Tang Z, Chen M, Chen T *et al.* FLNA and PGK1 are two potential markers for progression in hepatocellular carcinoma. *Cell Physiol Biochem* 2011; **27**: 207–216.
13 Bu Z, Liu R, Shang B, Cao Z, Pan Y, Zhou Q *et al.* A monoclonal antibody SZ-117 that recognizes filamin A derived from tumor cells. *Hybridoma* 2012; **31**: 214–218.
14 Bachmann AS, Howard JP, Vogel CW. Actin-binding protein filamin A is displayed on the surface of human neuroblastoma cells. *Cancer Sci* 2006; **97**: 1359–1365.
15 Heuze ML, Lamsoul I, Baldassarre M, Lad Y, Leveque S, Razinia Z *et al.* ASB2 targets filamins A and B to proteasomal degradation. *Blood* 2008; **112**: 5130–5140.
16 Feng Y, Chen MH, Moskowitz IP, Mendonza AM, Vidali L, Nakamura F *et al.* Filamin A (FLNA) is required for cell-cell contact in vascular development and cardiac morphogenesis. *Proc Natl Acad Sci USA* 2006; **103**: 19836–19841.
17 Hart AW, Morgan JE, Schneider J, West K, McKie L, Bhattacharya S *et al.* Cardiac malformations and midline skeletal defects in mice lacking filamin A. *Hum Mol Genet* 2006; **15**: 2457–2467.
18 Zhou X, Tian F, Sandzén J, Cao R, Flaberg E, Szekely L *et al.* Filamin B deficiency in mice results in skeletal malformations and impaired microvascular development. *Proc Natl Acad Sci USA* 2007; **104**: 3919–3924.
19 Zheng L, Baek HJ, Karsenty G, Justice MJ. Filamin B represses chondrocyte hypertrophy in a Runx2/Smad3-dependent manner. *J Cell Biol* 2007; **178**: 121–128.
20 Lu J, Lian G, Lenkinski R, De Grand A, Vaid RR, Bryce T *et al.* Filamin B mutations cause chondrocyte defects in skeletal development. *Hum Mol Genet* 2007; **16**: 1661–1675.
21 Rouhi P, Jensen LD, Cao Z, Hosaka K, Lanne T, Wahlberg E *et al.* Hypoxia-induced metastasis model in embryonic zebrafish. *Nat Protoc* 2010; **5**: 1911–1918.
22 Zhu TN, He HJ, Kole S, D'Souza T, Agarwal R, Morin PJ *et al.* Filamin A-mediated down-regulation of the exchange factor Ras-GRF1 correlates with decreased matrix metalloproteinase-9 expression in human melanoma cells. *J Biol Chem* 2007; **282**: 14816–14826.
23 Jurak Begonja A, Hoffmeister KM, Hartwig JH, Falet H. FlnA-null megakaryocytes prematurely release large and fragile platelets that circulate poorly. *Blood* 2011; **118**: 2285–2295.
24 Baldassarre M, Razinia Z, Brahme NN, Buccione R, Calderwood DA. Filamin A controls matrix metalloproteinase activity and regulates cell invasion in human fibrosarcoma cells. *J Cell Sci* 2012; **125**: 3858–3869.
25 Westermarck J, Kahari VM. Regulation of matrix metalloproteinase expression in tumor invasion. *FASEB J* 1999; **13**: 781–792.
26 Xu Y, Bismar TA, Su J, Xu B, Kristiansen G, Varga Z *et al.* Filamin A regulates focal adhesion disassembly and suppresses breast cancer cell migration and invasion. *J Exp Med* 2010; **207**: 2421–2437.
27 Caruso JA, Stemmer PM. Proteomic profiling of lipid rafts in a human breast cancer model of tumorigenic progression. *Clin Exp Met* 2011; **28**: 529–540.
28 Folkman J. Tumor angiogenesis: therapeutic implications. *N Engl J Med* 1971; **285**: 1182–1186.
29 Berardi S, Caivano A, Ria R, Nico B, Savino R, Terracciano R *et al.* Four proteins governing overangiogenic endothelial cell phenotype in patients with multiple myeloma are plausible therapeutic targets. *Oncogene* 2012; **31**: 2258–2269.
30 Del Valle-Perez B, Martinez VG, Lacasa-Salavert C, Figueras A, Shapiro SS, Takafuta T *et al.* Filamin B plays a key role in vascular endothelial growth factor-induced endothelial cell motility through its interaction with Rac-1 and Vav-2. *J Biol Chem* 2010; **285**: 10748–10760.
31 Zheng X, Zhou AX, Rouhi P, Uramoto H, Borén J, Cao Y *et al.* Hypoxia-induced and calpain-dependent cleavage of filamin A regulates the hypoxic response. *Proc Natl Acad Sci USA* 2014; **111**: 2560–2565.
32 Uramoto H, Akyürek LM, Hanagiri T. A positive relationship between filamin and VEGF in patients with lung cancer. *Anticancer Res* 2010; **30**: 3939–3944.
33 Hayashi K, Altman A. Filamin A is required for T cell activation mediated by protein kinase C-theta. *J Immunol* 2006; **177**: 1721–1728.
34 Tigges U, Koch B, Wissing J, Jockusch BM, Ziegler WH. The F-actin cross-linking and focal adhesion protein filamin A is a ligand and in vivo substrate for protein kinase Cα. *J Biol Chem* 2003; **278**: 23561–23569.
35 Kessenbrock K, Plaks V, Werb Z. Matrix metalloproteinases: regulators of the tumor microenvironment. *Cell* 2010; **141**: 52–67.
36 Zhou AX, Toylu A, Nallapalli RK, Nilsson G, Atabey N, Heldin CH *et al.* Filamin A mediates HGF/c-MET signaling in tumor cell migration. *Int J Cancer* 2011; **128**: 839–846.
37 Liu M, Sjögren AK, Karlsson C, Ibrahim MX, Andersson KM, Olofsson FJ *et al.* Targeting the protein prenyltransferases efficiently reduces tumor development in mice with K-RAS-induced lung cancer. *Proc Natl Acad Sci USA* 2010; **107**: 6471–6476.

Supplementary Information accompanies this paper on the Oncogenesis website (http://www.nature.com/oncsis)